Hydrogenation of Lactic Acid to 1,2-Propanediol over Ru-Based Catalysts

Kaituo Liu,[a] Xiaoming Huang,[a] Evgeny A. Pidko,*[b, c] and Emiel J. M. Hensen*[a]

The catalytic hydrogenation of lactic acid to 1,2-propanediol with supported Ru catalysts in water was investigated. The influence of catalyst support (activated carbon, γ-Al$_2$O$_3$, SiO$_2$, TiO$_2$, and CeO$_2$) and promoters (Pd, Au, Mo, Re, Sn) on the catalytic performance was evaluated. Catalytic tests revealed that TiO$_2$ yields the best Ru catalysts. With a monometallic Ru/TiO$_2$ catalyst, a 1,2-propanediol yield of 70 % at 79 % lactic acid con-

version was achieved at 130 °C after 20 h reaction. Minor by-products of the hydrogenation reaction were propionic acid, ethanol, 1-propanol, and 2-propanol. For the bimetallic catalysts, the addition of Pd and Au slightly enhanced the performance of Ru/TiO$_2$, whereas the addition of common hydrogenation promoters such as Re, Mo, and Sn impaired the activity.

Introduction

Lignocellulosic biomass is a potential low-cost and renewable carbon source for the chemical industry.[1] A common approach to valorize biomass is its conversion to platform chemicals, which then serve as the starting chemicals for further applications. Lactic acid (LA) is a recognized biobased platform molecule,[2] which is commonly produced by fermentation. Given sustainability issues with this enzymatic route, there is also significant interest in obtaining lactic acid by chemocatalytic approaches.[3] Polymerization of a homochiral LA via the intermediate formation of the cyclic lactide molecules results in polylactic acid (PLA), a biobased and biodegradable plastic.[4] Dehydration of LA at the α-hydroxyl position yields acrylic acid, which is the primary monomer for the synthesis of acrylate polymers.[5] The oxidative dehydrogenation of LA gives pyruvic acid, which finds diverse applications in food, cosmet-

ics, and pharmaceutical industries.[6, 7] Other important LA conversion routes include decarboxylation to acetaldehyde,[8] condensation to 2,3-pentanedione,[9] and esterification to LA esters.[10]

The reductive transformation of LA to 1,2-propanediol (1,2-PDO) through catalytic hydrogenation is regarded as an attractive green alternative to the current process in which 1,2-PDO is obtained through the hydration of propylene oxide.[11] The main challenge in establishing a catalytic process for the hydrogenation of LA to 1,2-PDO is to reduce the carboxylic acid group, while preserving the α-hydroxy moiety. Given the intrinsic difficulty to reduce carboxylic acids with H$_2$, harsh conditions are typically required to achieve high conversion,[12] which usually has the drawback of also promoting undesired hydrogenolysis side reactions. The development of an active catalyst for selective hydrogenation of LA to 1,2-PDO under mild reaction conditions is highly desired.[13]

Hydrogenation of LA using heterogeneous catalysts has been discussed since the 1950s. Neat lactic acid could be successfully reduced in the presence of a Re black at 150 °C and 258 bars of H$_2$, yielding up to 80 % of 1,2-PDO.[14] The hydrogenation of LA in the gas phase has been reported using a Cu-based catalyst at temperatures between 160 °C and 220 °C, resulting in high 1,2-PDO yields.[12, 15] Supported Ru has been recently identified as a promising catalyst for the aqueous-phase hydrogenation of carbonyl-containing biomass-derived oxygenates including carboxylic acids.[16] The activity of Ru can be promoted by Sn or Mo to enable the selective hydrogenation of carboxylic acids and their esters.[17] Earlier studies on the hydrogenation of aqueous lactic acid identified carbon-supported Ru catalysts as active and highly selective catalysts.[18] However, the optimal performance of such catalysts could only be established at a H$_2$ pressure as high as 140 bar. Subsequent studies mainly focused on reducing the temperature and pressure requirements for the hydrogenation process and the most representative results are summarized in Table 1.[19–23]

[a] K. Liu, Dr. X. Huang, Prof. Dr. E. J. M. Hensen
Laboratory of Inorganic Materials Chemistry,
Schuit Institute of Catalysis
Eindhoven University of Technology
P.O. Box 513, 5600 MB Eindhoven (The Netherlands)
E-mail: e.j.m.hensen@tue.nl

[b] Prof. Dr. E. A. Pidko
ITMO University
Lomonosova str. 9, St. Petersburg 191002 (Russia)

[c] Prof. Dr. E. A. Pidko
Current address: Inorganic Systems Engineering group,
Department of Chemical Engineering
Delft University of Technology
Van der Maasweg 9, 2629 HZ Delft (The Netherlands)
E-mail: e.a.pidko@tudelft.nl

Supporting information and the ORCID identification number(s) for the author(s) of this article can be found under:
https://doi.org/10.1002/cctc.201701329.

Table 1. Overview of LA hydrogenation over Ru (5 wt.%) based catalyst in aqueous solution. C_0(LA), initial LA concentration; X(LA), conversion in %; S(1,2-PDO), selectivity to 1,2-PDO in %.

Catalyst	C_0(LA) [M]	P_{H_2} [bar]	T [°C]	t [h]	X(LA) [%]	S(1,2-PDO) [%]	Ref.
Ru/SiO$_2$	1	80	130	7	30	80	[19]
Ru/C	1	50	130	2	70	84	[20]
RuSn/C	1.66	60	190	4	>95	>95	[21]
Ru/C	0.55	35	120	2.5	19	>95	[22]
RuMoO$_x$/C	0.55	80	120	18	>95	95	[23]
Ru/C	0.55	80	120	2	13	93	[23]
Ru/SiO$_2$	0.55	80	120	2	4.7	92	[23]

Previous studies indicate that the highest 1,2-PDO selectivity can be obtained in the 110–200 °C temperature range. At higher temperatures, hydrogenolysis results in 1-propanol and 2-propanol. Furthermore, the solvent has a pronounced effect on the performance of the Ru catalysts. For TiO$_2$-supported catalysts, water has been identified as the preferred solvent.[24] Competitive adsorption of water with 1,2-PDO for surface sites and high solubility of the product in water shorten the residence time of the product on the catalyst surface, thereby limiting hydrogenolysis reactions.

In this work we performed a systematic study of LA hydrogenation by supported Ru catalysts. Particular attention was paid to the influence of the support and common hydrogenation promoters. For the best performing catalyst, the influence of the process conditions on 1,2-PDO selectivity was evaluated.

Results and Discussion

Catalyst identification

A series of 2 wt.% Ru catalysts supported on TiO$_2$ (P25), CeO$_2$, SiO$_2$, C, and γ-Al$_2$O$_3$ were prepared by incipient wetness impregnation. XRD patterns of the reduced catalysts are given in Figure 1a. The XRD patterns only contain features of the sup-
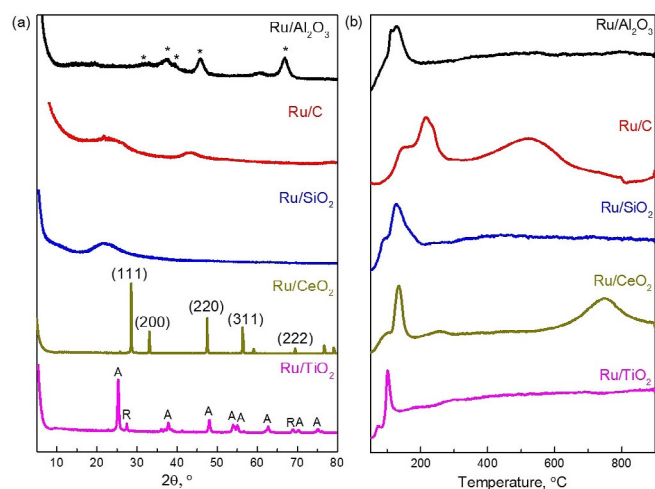
ports, implying the absence of large Ru and RuO$_2$ particles. Regarding the support features, XRD shows that TiO$_2$ is a mixture of anatase and rutile, CeO$_2$ has the fluorite structure, γ-Al$_2$O$_3$ gives rise to the well-known weak reflections of this semicrystalline oxide, and C and SiO$_2$ are X-ray amorphous. The textural properties of the catalysts are listed in Table 2. The highest surface area is obtained for the amorphous carbon support, the lowest for CeO$_2$.

Table 2. Physical–chemical properties of supported 2 wt.% Ru catalysts.

Catalyst	S_{BET} [m^{2}g^{-1}]	Pore volume [cm^{3}g^{-1}]	Average pore size [nm]
Ru/TiO$_2$	58	0.09	5.3
Ru/CeO$_2$	3	0.005	5.3
Ru/SiO$_2$	293	1.25	12.1
Ru/C	1470	0.37	2.9
Ru/Al$_2$O$_3$	192	0.54	7.6

The reducibility of the Ru supported catalysts was investigated by hydrogen temperature-programmed reduction (H$_2$-TPR). The TPR traces of the samples are shown in Figure 1b. The trace for Ru/TiO$_2$ shows a sharp reduction feature at 120 °C from the reduction of RuCl$_3$ to metallic Ru (Figure 1b). The position of this peak is shifted to lower temperature compared to the unsupported catalyst, for which the reduction peak is observed at approximately 155 °C,[25,26] suggesting that the TiO$_2$ support facilitates the reduction of RuCl$_3$. For the other catalysts, the main reduction feature is located at approximately 150 °C. The higher reducibility of Ru/TiO$_2$ may be explained by the acid–base characteristics of the TiO$_2$ surface which can catalyze the dissociation of H$_2$. Previous computational studies indicated the possibility of a heterolytic cleavage of H$_2$ at interfacial sites between Ru nanoparticles and basic bridging hydroxyl groups of the TiO$_2$ surface.[27] For Ru/C, besides the main peak at 150 °C, two additional reduction features at 200 °C and in the 400–600 °C range were observed. These peaks are most likely related to the reduction of oxygen-containing functional groups of the activated carbon surface.[28] For the Ru/CeO$_2$ sample, the broad peak at high temperature at 750 °C is attributed to the bulk reduction of the support.[29] The smaller feature below 300 °C is attributed to ceria surface reduction facilitated by hydrogen spilling over from the reduced Ru particles.

Representative TEM images of the reduced Ru catalysts are shown in Figure 2 along with the particle-size distribution and the average Ru particle size. Except for the low-surface-area ceria support ($d = 4.15$ nm), all catalysts contained on average smaller than 1 nm Ru particles.

The activity of the supported Ru catalysts was evaluated in the batch hydrogenation of aqueous 0.1 M LA at 130 °C. LA conversion and product yield obtained after 4 h are displayed in Figure 3. Ru/TiO$_2$ gave the highest 1,2-PDO yield (27%) at a LA conversion of 39%. The Ru/SiO$_2$, Ru/C, and Ru/Al$_2$O$_3$ catalysts were less active with 1,2-PDO yields of 11%, 21%, and 13%, respectively. Ru/CeO$_2$ was the least active and selective catalyst with only 3% yield of 1,2-PDO obtained at a LA con-
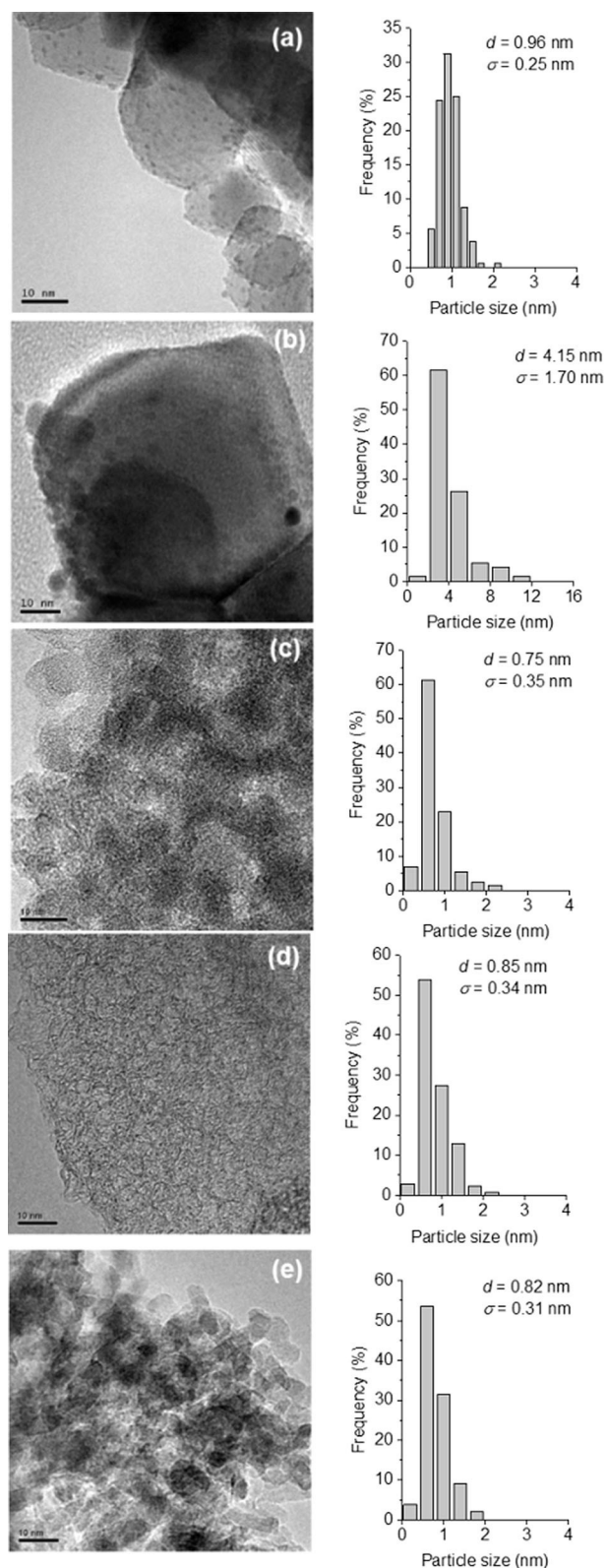

Figure 1. (a) XRD patterns and (b) TPR profiles of different supported 2 wt.% Ru catalysts (peak indications: A = anatase, R = rutile, * = γ-Al$_2$O$_3$).

Figure 2. TEM images of reduced (a) Ru/TiO$_2$, (b) Ru/CeO$_2$, (c) Ru/SiO$_2$, (d) Ru/C, and (e) Ru/γ-Al$_2$O$_3$ catalysts.(Ru loading: 2 wt.%).
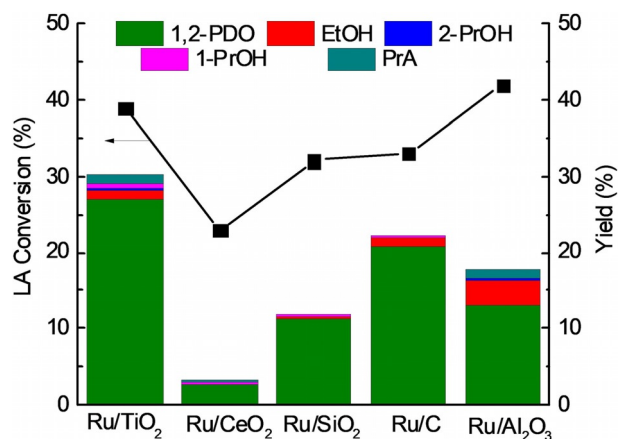

Figure 3. LA conversion (left) and product yield (right) for the 2 wt.% Ru catalysts (conditions: 0.1 M LA, 130 °C, 4 h, 40 bar H$_2$).

pared to the mixed-phase P25-supported catalyst (Supporting Information, Figure S3). The origin of such a different activity behavior is not clear and will be investigated in our further studies. The low activity of Ru/CeO$_2$ is likely attributable to the large Ru particle size. The superior activity of the P25 TiO$_2$-supported catalysts is tentatively attributed to their high reducibility. TPR data reveals that Ru nanoparticles supported on P25 TiO$_2$ are reduced already at 120 °C, which allows maintaining their reduced state under the conditions of the catalytic reaction (130 °C). Previous studies also highlight the importance of specific Lewis acidity of the TiO$_2$ support that additionally polarizes the carbonyl group of LA making it more susceptible to reduction over the Ru nanoparticles.[17b, 30]

For all catalysts, byproducts obtained in relatively small amounts were propionic acid (PrA), ethanol (EtOH), 1-propanol (1-PrOH), and 2-propanol (2-PrOH). For Ru/TiO$_2$, the overall yield of these byproducts was approximately 3%. Gas-phase analysis of the gas cap of the experiment with Ru/TiO$_2$ (Supporting Information, Table S1) revealed the formation of small quantities of alkanes such as CH$_4$ (0.3%, carbon yield), C$_2$H$_6$ (0.1%), and C$_3$H$_8$ (1.0%). No CO and only negligible amounts of CO$_2$ were detected. The overall yield of these gaseous products was 1.4%. Similar amounts of gaseous products were formed with the other catalysts. Importantly, the carbon balance for LA conversion could not be closed for the experiments with Ru/CeO$_2$, Ru/SiO$_2$, and Ru/Al$_2$O$_3$. The conversion of LA was substantially higher than the total yield of analyzed liquid products. The difference cannot be accounted for by the small amounts of gaseous products. We were not able to identify the products responsible for this loss of carbon neither by the chromatography nor by ^{1}H NMR spectroscopy, in which all major peaks were identified and quantified.

Catalyst optimization

Having identified TiO$_2$-supported Ru as the most promising catalyst for the selective hydrogenation of LA to 1,2-PDO, we aimed to optimize the performance towards Ru loading and by using promoters.

version of 23%. We also tested Ru supported on pure-phase anatase and rutile, as well as the high-surface-area CeO$_2$ (150 m^2 g^{-1}). They were all found to be nearly inactive com-

Firstly, we optimized the Ru loading of the Ru/TiO$_2$ catalyst. Representative TEM images of the reduced catalysts are shown in Figure 4. The catalysts containing 5 wt.% and 8 wt.% Ru contain on average 1.9 ± 0.7 nm and 1.8 ± 0.8 nm particles. Increasing the loading to 10 wt.% Ru resulted in nanoparticles with an average size of 2.2 ± 1.2 nm. Thus, increasing the loading leads to a modest increase of the particle size from about 1 to 2 nm with a concomitant broadening of the particle-size distribution.
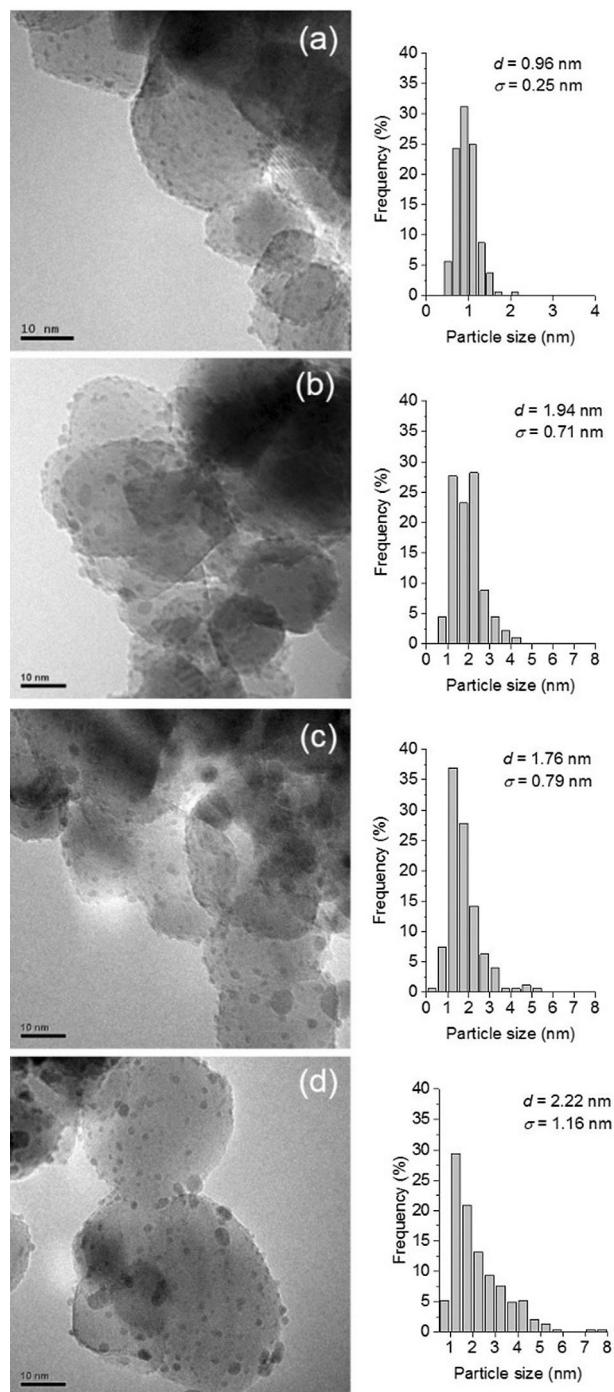
LA hydrogenation data for these catalysts are shown in Figure 5. The LA conversion and 1,2-PDO yield display a maximum at a Ru content of 8 wt.%. Notably, the carbon balance for the experiments for the 5 wt.% and 8 wt.% catalysts was
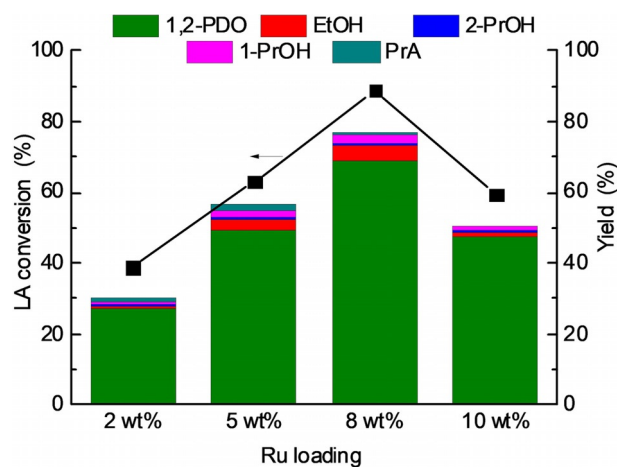
Figure 5. LA conversion (left) and product yield (right) for Ru/TiO$_2$ with different Ru loadings (conditions: 0.1 M LA, 130 °C, 4 h, 40 bar H$_2$).

closed. Although the 8 wt.% Ru/TiO$_2$ resulted in the highest 1,2-PDO yield of 70%, it also catalyzed the formation of ethanol, 1-propanol, and 2-propanol in larger amounts than the 2 wt.% catalyst. By normalizing the 1,2-PDO yields to the total Ru contents, turnover number (TON) values can be estimated to be 34, 28, 25, and 13 for Ru/TiO$_2$ containing 2, 5, 8, and 10 wt.% Ru, respectively. These data suggest that the intrinsic activity of the catalyst remains almost the same until 8 wt.% Ru loading. The increase of the particle size observed at higher Ru loading is accompanied by a substantial drop in the intrinsic activity, suggesting a pronounce structure sensitivity of the hydrogenation reaction with optimum activity towards 1,2-PDO formation obtained for the intermediately sized Ru nanoparticles.

Although high-loading Ru/TiO$_2$ catalyst gave a higher 1,2-PDO yield, this catalyst also leads to more byproducts. With the goal of further improving the activity and selectivity of the Ru/TiO$_2$ catalyst, we explored the influence of metal promoters. Previous studies have shown that the formation of alloyed nanoparticles can enhance the catalyst activity by modifying the electronic or structural properties of the active phase.[31] For instance, Sn has been widely studied as an additive to hydrogenation catalysts and it might also play a role in activating the carboxyl group in carboxylic acid reactants.[21,30a] The formation of bimetallic RuPd nanoparticles resulted in a superior hydrogenation activity (99% selectivity towards γ-valerolactone in the hydrogenation of levulinic acid) owing to the dilution and isolation of the active Ru sites by Pd.[32] Bimetallic RuAu/C improved the activity and stability in LA hydrogenation.[33]

Inspired by these earlier studies, we prepared several bimetallic RuM/TiO$_2$ with M = Mo, Sn, Re. The Ru loading was kept at 2 wt.%, and the atomic amount of promoter was the same as that of Ru.

Figure 4. TEM images of (a) 2 wt.% Ru/TiO$_2$, (b) 5 wt.% Ru/TiO$_2$, (c) 8 wt.% Ru/TiO$_2$, and (d) 10 wt.% Ru/TiO$_2$, and the corresponding particle-size-distribution histograms.

The XRD patterns of the bimetallic catalysts are shown in Figure 6. Only the diffraction peaks of rutile and anatase phases of the support were observed, indicative of the high dispersion of the metallic phase. Only for the RuAu catalyst, small features from the presence of gold particles with an estimated size in the 5–10 nm range were observed.
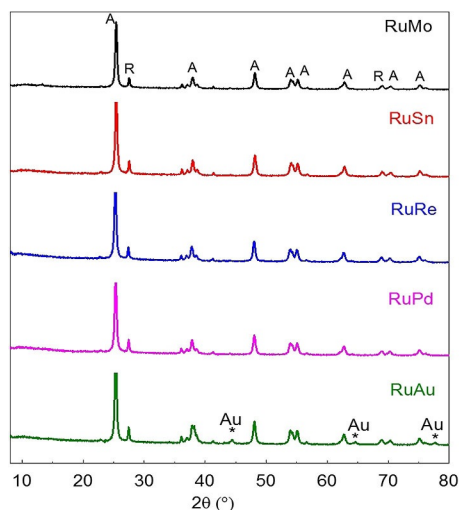

Figure 6. XRD patterns of the Ru-based bimetallic catalysts supported on TiO$_2$ (loadings: Ru 2 wt.%, Mo 1.9 wt.%, Sn 2.4 wt.%, Re 3.7 wt.%, Pd 2.1 wt.%, Au 3.9 wt.%).

The results of the catalytic tests with the RuM/TiO$_2$ catalysts are presented in Figure 7. The addition of Au did not have a significant effect on the catalytic performance. A slightly higher LA conversion (45%) was obtained with the RuAu/TiO$_2$ compared to the monometallic counterpart (39%), whereas the 1,2-PDO yield (29%) was the same. Similarly, the addition of Pd and Re did not substantially affect the 1,2-PDO yield, despite the higher activity of the RuPd catalyst. The increased LA conversion was accompanied by a decreased 1,2-PDO selectivity. The decreased 1,2-PDO selectivity was caused by the enhanced hydrogenolysis reactions as evident from the increased
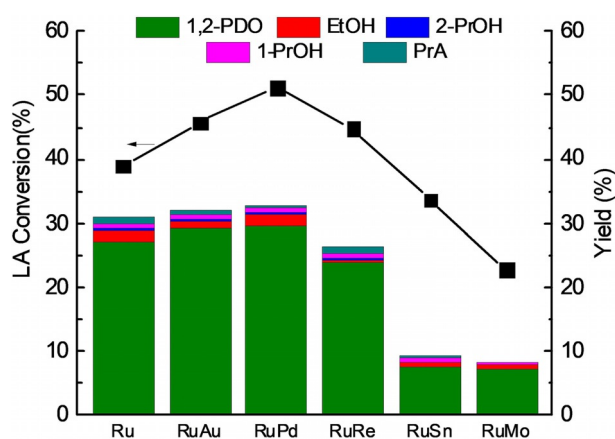
selectivity to 1-propanol and 2-propanol. This conclusion is also supported by the higher yields of gaseous products (Supporting Information, Table S1). The addition of Sn and Mo had a strong negative effect on the catalytic performance, especially with respect to LA conversion. Based on these data, we conclude that promoters do not bring a real advantage. Therefore, we further investigated the influence of the reaction parameters such as reaction time and temperature for the 2 wt.% Ru/TiO$_2$ catalyst. We attribute the observed lack of activity enhancement in the current bimetallic catalyst formulations to the current choices of the synthesis methodology and loading of the promoters, as well as other parameters of the synthesis. In this work, we selected the co-impregnation method for the preparation of the bimetallic catalysts to achieve a high loading of the promoter. Previously, this method was successfully employed by us for the preparation of a wide range of Re-promoted Ni[34] and Pd hydrogenation catalysts. Other synthesis approaches could have led to more active systems. For example, Jong-Min Lee and co-authors successfully employed a sequential coprecipitation–deposition method to prepare RuSn/ZnO catalysts showing an exceptional activity in the hydrogenation of butyric acid to n-butanol[35] Takeda et al. employed a sequential impregnation method to a highly active Ru–MoO$_x$/SiO$_2$ material capable of hydrogenating LA at 120°C and 80 bar H$_2$.[23]

Process conditions optimization

The results of the catalytic tests at varied reaction times at 130°C with 2 wt.% Ru/TiO$_2$ catalyst are presented in Figure 8. Similarly to the above findings, the increase of LA conversion with the reaction time led to a pronounced increase in 1,2-PDO selectivity and an improved carbon balance. After 20 h reaction time at 130°C, 70% yield of 1,2-PDD at 79% LA conversion was obtained along with a nearly complete carbon balance.

Next, we evaluated the influence of the reaction temperature on the outcome of the catalytic reaction with 2 wt.% Ru/TiO$_2$ catalyst. The results of the catalytic experiments are given
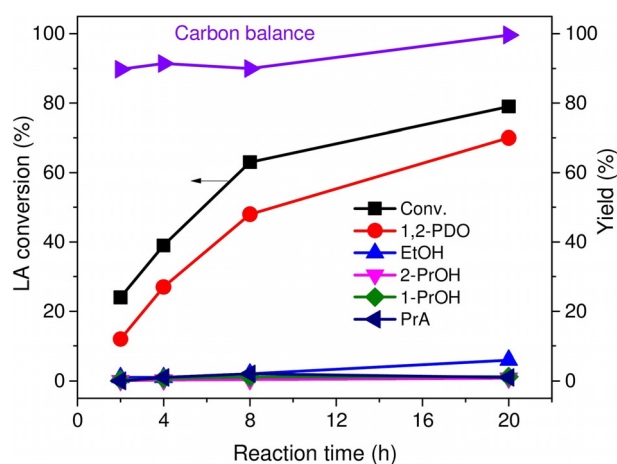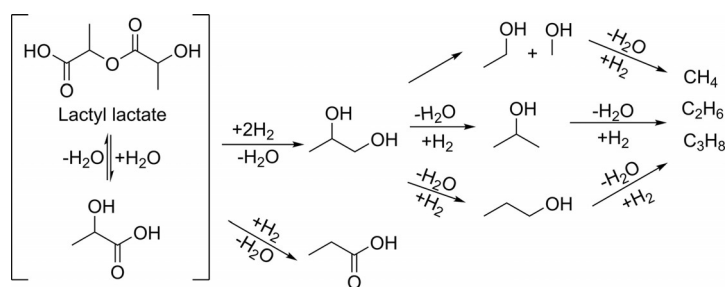

Figure 7. LA conversion (left) and product yield (right) for RuM/TiO$_2$ catalysts (conditions: 0.1 M LA, 130°C, 4 h, 40 bars H$_2$; loadings: Ru 2 wt.%, Mo 1.9 wt.%, Sn 2.4 wt.%, Re 3.7 wt.%, Pd 2.1 wt.%, Au 3.9 wt.%).

Figure 8. LA conversion (left) and product yield (right) for 2 wt.% Ru/TiO$_2$ as a function of reaction time (conditions: 0.1 M LA, 130°C, 40 bar H$_2$).

in Figure 9. Expectedly, the reaction at 110 °C gave only a low LA conversion of approximately 27 % with a 1,2-PDO yield of 14 %. The increase of the reaction temperature up to 180 °C resulted in a simultaneous increase of both the LA conversion and 1,2-PDO yield. A maximum 1,2-PDO yield of 64 % at 84 % LA conversion was obtained in 4 h reaction time at 180 °C. The high conversion resulted in a higher overall yield (13 %) of the monoalcohol hydrogenolysis products as well as the short-chain alkanes in the gas phase (8 %, Table S1). Further in-

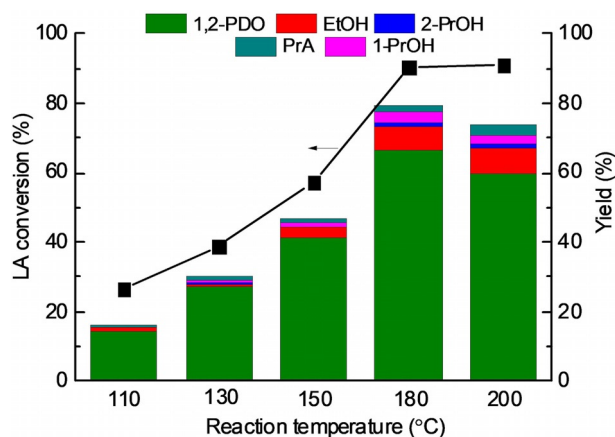**Scheme 1.** Possible reaction pathways for LA hydrogenation in water.

Figure 9. LA conversion (left) and product yield (right) for 2 wt. % Ru/TiO$_2$ as a function of reaction temperature (conditions: 0.1 M LA, 4 h, 40 bar H$_2$).

crease of the reaction temperature to 200 °C led to a pronounced decrease of the yield of the target 1,2-PDO product suggesting the range between 130 °C and 180 °C to be optimal for the catalytic LA hydrogenation with Ru/TiO$_2$.

We performed additional LA hydrogenation reactions by varying the pressure from 10 to 40 bar at 180 °C for 4 h with the 2 wt. % Ru/TiO$_2$ catalyst. It was found that the yield of 1,2-PDO linearly increases with increasing reaction pressure (Figure S4). This is in line with earlier studies demonstrating that the formation of 1,2-PDO is generally favored at a higher pressure,[15a] at least in part because of the strong pressure dependency of H$_2$ solubility in water.[19] The increase of the LA feed concentration five-fold to 0.5 M while keeping the LA/Ru ratio similar to that of the other tests did not affect substantially the reaction outcome. A similar 1,2-PDO yield of 68 % at 84 % LA conversion could be obtained after 4 h reaction at 180 °C. An appropriate amount of spent catalyst was weighed and utilized in a next catalytic test following the standard procedure (20 mg catalyst, 0.1 M LA). In this recycling experiment, an 1,2-PDO yield of 64 % was obtained similarly to that in the catalytic test employing the fresh catalyst.

Mechanistic proposal

Based on the product distributions observed in the catalytic tests, we put forward a proposal for the mechanism of LA conversion over Ru/TiO$_2$ catalyst (Scheme 1). The commercial

90 wt. % LA aqueous solution contains some lactyl lactate and this dimer will hydrolyze to form LA under the reaction conditions. Hydrogenation of carboxylic acid group of LA yields 1,2-PDO as the major product. One side reaction is the nonselective hydrogenolysis of the α-OH group of the LA to yield propionic acid. Another side reaction is the consecutive hydrogenolysis of the 1,2-PDO, yielding 1-propanol and 2-propanol.[36] Further hydrogenolysis of these alcohols results in the formation of C$_3$ alkanes. Ethanol can be obtained through decarboxylation of LA. However, only trace amount of CO$_2$ was detected during reactions, suggesting that decarboxylation might not be the path for ethanol formation. Given the high yield of methane, we believe that ethanol is likely formed by C—C bond cleavage of 1,2-PDO. In this way, ethanol was produced together with methanol followed by a fast conversion of methanol to methane.

Conclusions

Supported monometallic and bimetallic Ru-based catalysts were synthesized and tested in the aqueous phase hydrogenation of lactic acid (LA) to 1,2-propanediol (PDO). The XRD and TEM characterizations showed that the metal particles are highly dispersed on TiO$_2$ surface. Ru/TiO$_2$ gave the lowest reduction temperature compared to other supports, which makes it an excellent support for the hydrogenation of LA. The addition of different metal promoters to the Ru catalyst did not result in substantial activity enhancement and, accordingly, optimization of the reaction conditions and catalyst formulation was performed with the Ru/TiO$_2$ system. The catalyst shows a pronounced hydrogenation activity at the temperature as low as 130 °C. The optimal performance was established at this temperature allowing to reach a 1,2-PDO yield of 70 % and LA conversion of 79 %. Further increase of the temperature led to pronounced selectivity decline attributable to several side-reactions.

Experimental Section

Materials and methods.

Lactic acid (LA, 90 wt. % aqueous solution), 1,2-propandiol (1,2-PDO, 98 %), 1-propanol (99 %), 2-propanol (99 %), ethanol (99 %), and propionic acid (99 %) were purchased from Sigma–Aldrich. Ruthenium(III) chloride hexahydrate (38 wt. % Ru) was purchased from VWR. Amorphous SiO$_2$ (481 m^2 g^{-1}), γ-Al$_2$O$_3$ (231 m^2 g^{-1}), CeO$_2$,

and TiO$_2$ (P25, 50 m^2 g^{-1}), and commercial 5 wt.% Ru/C were purchased from Sigma–Aldrich. H$_2$ (99.999%) and N$_2$ (99.999%) were purchased from Linde Gas. All the reagents were used as received without further purification. MilliQ water was used in the preparation of catalysts, reactor feeds, calibration standards, and HPLC mobile phases.

Catalyst preparation

Catalyst comprised of Ru supported on TiO$_2$ (P25), CeO$_2$, SiO$_2$, C, and γ-Al$_2$O$_3$ were prepared by incipient wetness impregnation using RuCl$_3$·xH$_2$O (38 wt.% Ru) as the metal precursor. The loading of ruthenium was fixed at 2 wt.% on these supports. All the supports were dried at 110 °C for 24 h before impregnation. For the preparation of monometallic Ru-based catalysts, milliQ water (3 mL g^{-1} catalyst) was added into the amount of Ru precursor needed. For the bimetallic catalysts (RuM/TiO$_2$), the metal precursor was added to the Ru precursor solution. The loading of ruthenium was fixed at 2 wt.%. The second metal was added with the molar ratio to Ru of 1:1. The specific loadings of the second metals are summarized in Table S2. The precursor solution was stirred at 300 rpm for 10 min before adding it to the support. Then, the slurries were stirred for 4 h at 250 rpm and predried in a sand bath at 80 °C followed by drying in an oven overnight at 110 °C. Finally, the catalysts were reduced in a H$_2$/N$_2$ (v/v 10/90, 1.00 mL min^{-1}) at 350 °C for 2 h after heating at a rate of 2 °C min^{-1}.

Catalyst characterization

Crystal phase analysis of the reduced catalysts was performed on a Bruker Phaser 2 X-ray powder diffraction (XRD) apparatus using Cu$_{K\alpha}$ radiation source (2θ range from 5° to 80°). Textural analysis was performed by N$_2$ physisorption performed on a Tristar 3000 automated gas adsorption system. Prior to analysis, samples were degassed at 300 °C for 6 h. TPR experiments were performed in a flow apparatus equipped with a fixed-bed reactor, a computer-controlled oven, and a thermal conductivity detector. Typically, the catalyst (50 mg) was loaded into a tubular quartz reactor. Before TPR, samples were pretreated at 150 °C for 2 h. The sample was reduced in 4 vol.% H$_2$ in N$_2$ at a flow rate of 8 mL min^{-1}, whilst heating from room temperature up to 900 °C. The H$_2$ signal was calibrated using a CuO/SiO$_2$ reference catalyst. TEM was used to determine the average Ru particle size and the particle size distribution for the reduced catalysts. To this end, a catalyst sample was suspended in excess ethanol by sonication, and aliquots were deposited on 300 mesh carbon film Cu grids (EMS) and dried overnight under ambient conditions. Images were taken by using a JEOL 2010F equipped with a Schottky field emission gun operated at 200 kV and a Gatan CCD camera. Particle-size distributions were extracted from the TEM images using image processing software (ImageJ).

Catalytic activity testing

Aqueous-phase catalytic hydrogenation of LA to 1,2-PDO was performed in a 10 mL autoclave (HOKE Swagelok) at various reaction temperatures (110 °C–180 °C) and a (cold) hydrogen pressure of 40 bar. Typically, 0.1 M LA aqueous solution (5 mL) and reduced catalyst (20 mg) were charged into the autoclave in a nitrogen-flushed glove box. The sealed autoclave was then purged 4 times with H$_2$ before it was pressurized at 40 bar with H$_2$ at room temperature. Typically, the autoclave was heated at 130 °C and stirred at 1100 rpm (magnetic stirring). After the reaction, the heater was re-moved, and the autoclave was rapidly cooled in an ice bath. The gaseous products (methane, ethane, propane, CO$_2$, CO) were analyzed by an off-line Interscience Compact GC. After the remaining gaseous products were released, the liquid product was separated from the catalyst by filtration (syringe filter 0.45 μm, VWR International) and transferred to a glass vial.

Product analysis

Quantitative analysis of the liquid products was performed by a combination of HPLC and ^{1}H NMR spectroscopy. The concentrations of LA and propionic acid were quantified by using a Shimadzu HPLC equipped with a Prevail Organic Acid column and UV detector. Phosphate buffer (25 mM, pH 2) was used as mobile phase to ensure that all acidic groups of the compounds were protonated. All the liquid samples were directly subjected to analysis without dilution. Analysis showed that the commercially obtained aqueous solution of 90 wt.% LA contains LA monomer, lactyl lactate dimers, and oligomers. The composition depends on the LA concentration. In this work, a 0.1 M aqueous LA solution was used as the starting material.

Quantitative analysis of LA solutions with ^{1}H and ^{1}H–^{13}C nuclear magnetic resonance measurements revealed that the starting 0.1 M solution contains 72.1 wt.% LA, 27.4 wt.% dimer (lactyl lactate), and 0.5 wt.% oligomers (see the supporting information). No cyclic lactide was observed in the solution (Supporting Information, Figure S1). The dimer was completely hydrolyzed to form LA monomer after heating at 130 °C for 4 h in water without a catalyst (Figure S2). Therefore, to simplify the data presentation we assumed that the 0.1 M LA solution feed only contained LA monomer. Given that the dimer totally disappeared after the reaction, the concentration of the remaining LA monomer as determined by HPLC was used for calculating the reaction conversion. The quantification of LA and propionic acid were made based on the calibration curves generated with authentic compound solutions in HPLC.

^{1}H NMR was used for the quantification of the other liquid products including 1,2-PDO, ethanol,1-propanol, and 2-propanol. For the preparation of NMR samples, a 0.25 mL volume of the liquid solution was added into a 5 mm NMR sample tube together with 0.25 mL water and 0.05 mL deuterated dimethylsulfoxide-d_6 ([D$_6$]DMSO) solvent, which contained 2 mg mL^{-1} 1,4-dioxane as the internal standard. For quantitative ^{1}H NMR analysis, 32 scans were averaged using a relaxation delay of 5 s. All spectra were integrated by using the MestReNova software.

The conversion of LA (X) was calculated as follows: [Eq. (1)]

$$X(\%) = \frac{C_{LA,0} - C_{LA}}{C_{LA,0}} \times 100\% \qquad (1)$$

The yield of the liquid component i (Y_i) was calculated as follows: [Eq. (2)]

$$Y_i(\%) = \frac{C_{product\ i}}{C_{LA,0}} \times 100\% \qquad (2)$$

The gaseous product (methane, ethane, propane, CO$_2$, CO) were analyzed by an Interscience Compact GC system, equipped with Molsieve 5 Å and Porabond Q columns employing a thermal conductivity detector (TCD) and an Al$_2$O$_3$/KCl column with a flame ionization detector (FID).

Acknowledgements

Conflict of interest

The authors declare no conflict of interest.

[1] P. Balla, V. Perupogu, P. K. Vanama, V. R. C. Komandur, *J. Appl. Chem. Biotechnol.* **2016**, *91*, 769–776.

[2] Y. Fan, C. Zhou, X. Zhu, *Catal. Rev.* **2009**, *51*, 293–324.

[3] a) M. Dusselier, P. Van Wouwe, A. Dewaele, E. Makshina, B. F. Sels, *Energy Environ. Sci.* **2013**, *6*, 1415–1442; b) K. Liu, A. Litke, Y. Su, B. G. van Campenhout, E. A. Pidko, E. J. M. Hensen, *Chem. Commun.* **2016**, *52*, 11634–11637.

[4] M. Dusselier, P. Van Wouwe, A. Dewaele, P. A. Jacobs, B. F. Sels, *Science* **2015**, *349*, 78–80.

[5] B. Yan, L.-Z. Tao, Y. Liang, B.-Q. Xu, *ACS Catal.* **2014**, *4*, 1931–1943.

[6] S. Lomate, T. Bonnotte, S. Paul, F. Dumeignil, B. Katryniok, *J. Mol. Catal. A* **2013**, *377*, 123–128.

[7] N. Maleki, M. Eiteman, *Fermentation* **2017**, *3*, 8–24.

[8] C. Tang, J. Peng, X. Li, Z. Zhai, W. Bai, N. Jiang, H. Gao, Y. Liao, *Green Chem.* **2015**, *17*, 1159–1166.

[9] G. C. Gunter, D. J. Miller, J. E. Jackson, *J. Catal.* **1994**, *148*, 252–260.

[10] D. J. Benedict, S. J. Parulekar, S.-P. Tsai, *Ind. Eng. Chem. Res.* **2003**, *42*, 2282–2291.

[11] T. A. Nijhuis, M. Makkee, J. A. Moulijn, B. M. Weckhuysen, *Ind. Eng. Chem. Res.* **2006**, *45*, 3447–3459.

[12] M. N. Simonov, I. L. Simakova, V. N. Parmon, *React. Kinet. Catal. Lett.* **2009**, *97*, 157–162.

[13] P. Mäki-Arvela, I. L. Simakova, T. Salmi, D. Y. Murzin, *Chem. Rev.* **2014**, *114*, 1909–1971.

[14] H. S. Broadbent, G. C. Campbell, W. J. Bartley, J. H. Johnson, *J. Org. Chem.* **1959**, *24*, 1847–1854.

[15] a) R. D. Cortright, M. Sanchez-Castillo, J. A. Dumesic, *Appl. Catal. B* **2002**, *39*, 353–359; b) M. N. Simonov, I. L. Simakova, T. P. Minyukova, A. A. Khassin, *Russ. Chem. Bull.* **2009**, *58*, 1114–1118.

[16] J. Lee, Y. Xu, G. W. Huber, *Appl. Catal. B* **2013**, *140–141*, 98–107.

[17] a) R. Pestman, R. M. Koster, J. A. Z. Pieterse, V. Ponec, *J. Catal.* **1997**, *168*, 255–264; b) A. Primo, P. Concepcion, A. Corma, *Chem. Commun.* **2011**, *47*, 3613–3615; c) M. Toba, S. Tanaka, S. Niwa, F. Mizukami, Z. Koppany, L. Guczi, K. Y. Cheah, T. S. Tang, *Appl. Catal. A* **1999**, *189*, 243–250; d) H. G. Manyar, C. Paun, R. Pilus, D. W. Rooney, J. M. Thompson, C. Hardacre, *Chem. Commun.* **2010**, *46*, 6279–6281.

[18] Z. Zhang, J. E. Jackson, D. J. Miller, *Appl. Catal. A* **2001**, *219*, 89–98.

[19] T. Y. Jang, K. B. Chung, H. R. Eom, D. K. Noh, I. K. Song, J. Yi, S.-H. Baeck, *Res. Chem. Intermed.* **2011**, *37*, 1275–1282.

[20] H. Jang, S.-H. Kim, D. Lee, S. E. Shim, S.-H. Baeck, B. S. Kim, T. S. Chang, *J. Mol. Catal. A* **2013**, *380*, 57–60.

[21] S. Akiyama, T. Kakio, S. Indou, R. Oikawa, K. Ugou, R. Hiraki, M. Sano, T. Suzuki, T. Miyake, *J. Jpn. Pet. Inst.* **2014**, *57*, 216–224.

[22] S. Iqbal, S. A. Kondrat, D. R. Jones, D. C. Schoenmakers, J. K. Edwards, L. Lu, B. R. Yeo, P. P. Wells, E. K. Gibson, D. J. Morgan, C. J. Kiely, G. J. Hutchings, *ACS Catal.* **2015**, *5*, 5047–5059.

[23] Y. Takeda, T. Shoji, H. Watanabe, M. Tamura, Y. Nakagawa, K. Okumura, K. Tomishige, *ChemSusChem* **2015**, *8*, 1170–1178.

[24] G.-Y. Fan, Y. Zhang, Y.-F. Zhou, R.-X. Li, H. Chen, X.-J. Li, *Chem. Lett.* **2008**, *37*, 852–853.

[25] P. Betancourt, A. Rives, R. Hubaut, C. E. Scott, J. Goldwasser, *Appl. Catal. A* **1998**, *170*, 307–314.

[26] P. G. J. Koopman, A. P. G. Kieboom, H. van Bekkum, *J. Catal.* **1981**, *69*, 172–179.

[27] R. C. Nelson, B. Baek, P. Ruiz, B. Goundie, A. Brooks, M. C. Wheeler, B. G. Frederick, L. C. Grabow, R. N. Austin, *ACS Catal.* **2015**, *5*, 6509–6523.

[28] X. Yang, X. Wang, J. Qiu, *Appl. Catal. A* **2010**, *382*, 131–137.

[29] H. C. Yao, Y. F. Y. Yao, *J. Catal.* **1984**, *86*, 254–265.

[30] a) J. Pritchard, G. A. Filonenko, R. van Putten, E. J. M. Hensen, E. A. Pidko, *Chem. Soc. Rev.* **2015**, *44*, 3808–3833; b) M. J. Mendes, O. A. A. Santos, E. Jordão, A. M. Silva, *Appl. Catal. A* **2001**, *217*, 253–262.

[31] H. Jahangiri, J. Bennett, P. Mahjoubi, K. Wilson, S. Gu, *Catal. Sci. Technol.* **2014**, *4*, 2210–2229.

[32] W. Luo, M. Sankar, A. M. Beale, Q. He, C. J. Kiely, P. C. Bruijnincx, B. M. Weckhuysen, *Nat. Commun.* **2015**, *6*, 6540–6549.

[33] A. Villa, C. E. Chan-Thaw, S. Campisi, C. L. Bianchi, D. Wang, P. G. Kotula, C. Kubel, L. Prati, *Phys. Chem. Chem. Phys.* **2015**, *17*, 28171–28176.

[34] K. Liu, J. Pritchard, L. Lu, R. van Putten, M. W. G. M. Verhoeven, M. Schmitkamp, X. Huang, L. Lefort, C. J. Kiely, E. J. M. Hensen, E. A. Pidko, *Chem. Commun.* **2017**, *53*, 9761–9764.

[35] J. M. Lee, P. P. Upare, J. S. Chang, Y. K. Hwang, J. H. Lee, D. W. Hwang, D. Y. Hong, S. H. Lee, M. G. Jeong, Y. D. Kim, Y. U. Kwon, *ChemSusChem* **2014**, *7*, 2998–3001.

[36] Y. Amada, S. Koso, Y. Nakagawa, K. Tomishige, *ChemSusChem* **2010**, *3*, 728–736.